Kovove Mater. 51 2013 275–281
DOI: 10.4149/km_2013_5_275

Residual stresses determination by neutron diffraction in a 100Cr6 chromium steel bearing ring

M. Rogante[1*] , G. Martinat[2], P. Mikula[3], M. Vrána[3]

[1]*Rogante Engineering Office, Contrada San Michele n. 61, 62012 Civitanova Marche, Italy*
[2]*SKF, 10060 Airasca, Italy*
[3]*Nuclear Physics Institute ASCR, v.v.i., 25068 Řež, Czech Republic*

Received 14 March 2012, received in revised form 19 March 2013, accepted 20 March 2013

Abstract

100Cr6 chrome steel submitted to martensitic hardening and tempering is usually adopted for particular industrial applications such as bearings, rings and rollers. These parts are often subjected to dynamic stresses in different fields of engineering and, consequently, it is important to know the residual stresses involved, especially in correspondence of critical zones, particularly fatigue-stress and/or crack sensitive.

In this paper, the residual stress investigation by neutron diffraction in a 100Cr6 chromium steel ring – before and after the introduction of a hub fixed by orbital rolling – is presented. The results supply information on the real residual stress status, showing its enhancement due to the installation of the hub and the successive rolling operation. The achieved data can support the manufacturing process in order to improve the life assessment of the considered component.

K e y w o r d s: 100Cr6 steel, rings, martensitic hardening, tempering, residual stress, neutron diffraction

1. Introduction

100Cr6 rings are normally used in various engineering sectors, where high dynamic stresses and particular stresses at the rolling contact are involved. The ever-increasing performance and requirements for these components call for an enhanced quality of the manufacturing procedure. These parts, thus, are purposely produced (e.g. from seamless tube manufactured by hot rolling and high hardened to 58–67 HRC) and then typically heat treated (e.g. hardening, annealing and tempering) to obtain specific properties as high strength, wear and corrosion resistance, dimensional stability and suitable magnetic properties. Special applications of these rings include the operation at high temperatures and fatigue conditions.

Advanced applications require higher operating efficiency, less sensitiveness to external load and better reliability under adverse conditions [1]. The results of the heat treatment (HT) performed can be influenced by various factors, which cannot be controlled by the HT process itself. Inhomogeneities in the ingot material, e.g., may create negative treatment properties concerning microstructure and/or distortion and this can direct to low process-capability factors, despite a high quality heat treatment. Distortion, in particular, can be increased due to various reasons, e.g., the presence of residual stresses (RS), which cause inhomogeneous relaxation at diverse sections of the microstructure [2]. The knowledge of RS produced during the final heat treatment step, as well as those induced in the last manufacturing phase before the heat treatment is very important, since the inhomogeneity of their distribution within a ring is the decisive parameter concerning the resulting distortion [3, 4]. The full manufacturing process, moreover, can be responsible for dimensional and shape variations as well as for micro- and nano-structure, phase transformations, geometry, chemical composition and RS. The austenite-martensite transformation, in particular, produces a volume expansion that contributes to the creation of RS. In this case the RS status, mainly related to those areas of the

*Corresponding author: tel./fax: +390733775248; e-mail address: main@roganteengineering.it

ring principally stress and/or crack receptive, plays a significant role. An ideal condition happens when favourable RS superimpose on elastic stresses, resulting in an improved fatigue life.

The main applications of 100Cr6 chromium steel are related to the automotive and mechanical engineering sectors, i.e., parts with required high hardness and excellent resistance to wear and deformation, such as balls, bearings, cams, rings and cold ring rolled products, rollers and helical springs. This material is very suitable, e.g., for the thixoforming process [5]. The quality of this steel is strictly connected with its micro- and nano-structure. Appropriate heat treatments allow lifetime enhancement, nevertheless, the eventual presence of residual austenite is able to reduce hardness, and hence the component lifetime. The rolling operation constrains the ring in the axial direction by shoulders on the rolls; cold ring rolling, moreover, can produce large deformations and important effects on microstructure and texture evolution [6, 7].

X-ray diffraction technique is routinely adopted as non-destructive method for in situ investigations of phase transformations, RS and texture changes in near-surface regions of industrial materials and parts. Nevertheless, X-ray diffraction supplies information from a small surface volume element and (according to the atomic number of the investigated material) allows to measure near surface RS only to the depth of a few hundred Å units and only in discrete locations. Moreover, any major surface damage like oxidation and decarburization can affect X-ray diffraction measurements: therefore, dissimilarities between theoretically and experimentally assessed values can be expected [7].

Neutrons have recently become an increasingly significant probe for materials across a wide range of disciplines. They have become more and more helpful in the characterization of materials and components of industrial interest when revealing significant properties related to the investigated objects [8–11]. Their speciality with respect to other techniques is the possibility of providing full information about the micro- and nano-physical structure of the material bulk and sub-surface in a non-destructive way. In the case of RS measurements, the main advantage of neutron diffraction over other methods is that it can provide required information in the depth from $\sim 50\,\mu m$ up to several centimetres with a spatial resolution being usually of 0.1–2 mm [8]. X-ray and neutron diffraction being mutually complementary then permit RS investigations from the surface to depth without any layer removal or hole drilling [12].

In the present experiment, neutron diffraction was used for determination of RS level in a chosen part of a ring made of 100Cr6 steel. Some other complementary studies related to bearing parts and 100Cr6 steel

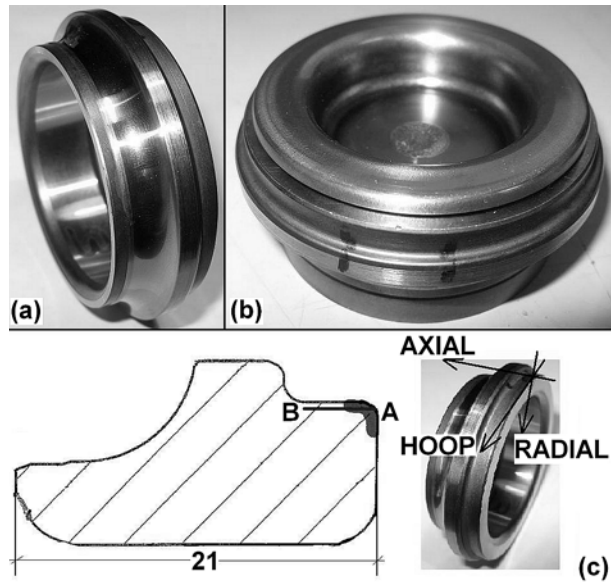

Fig. 1. Investigated rings and measurement details: free ring after manufacture (a), ring with the hub introduced (b), measurement stress components (c). Marked dimension is in mm.

via conventional methods – including mainly X-ray diffraction, scanning electron microscopy (SEM) and transmission electron microscopy (TEM) – have been carried out in the past and can be found in [13–19].

2. Materials and methods

2.1. Samples description

Figure 1 shows the investigated specimens and the measurement details. The free ring after manufacture (Fig. 1a) has an external diameter of $\sim$ 72 mm and an internal diameter of $\sim$ 52 mm. Through the ring a hub is introduced, which is fixed by the orbital rolling of the hub material. Figure 1b shows the ring joined with the hub. The introduction of the hub and the successive rolling operation increase the RS level in the ring: Figure 1c shows the critical zone in which a FEM analysis indicated a significant RS increase after the installation of the hub. Since this component is also submitted to in-service dynamic stresses, it is essential to determine the RS status, which can give useful information and guideline to improve the manufacturing process and enhance fatigue and crack resistance. For this purpose, the RS investigations were carried out on 3 samples: a ring without the hub (free ring), the same ring with the hub installed (completed ring), and in addition, for a possible comparison, one more completed ring have been investigated. The measurements were performed along the line AB indicated in Fig. 1 with reference to the three main directions (hoop, radial and axial).

Table 1. Chemical composition of the investigated UNI 100Cr6 steel rings, in wt.%

Element	C	Si	Mn	P	S	Cr	Mo	Cu	Al	O	Fe
min	0.93	0.15	0.25	–	–	1.35	–	–	–	–	bal.
max	1.05	0.35	0.45	0.025	0.015	1.60	0.10	0.30	0.050	0.0015	

The constitutive material of the ring is UNI 100Cr6 chromium alloy steel. Comparable international material grades are: AFNOR35-565 100Cr6; AISI/SAE 52100; ASTM A295-98 52100; DIN17230 100Cr6; EN 10027-2 1.3505; ISO 683-17:1999 steel type B1; JIS SUJ2; UNS G52986. The chemical composition of the analysed rings is reported in Table 1.

This steel exhibits high hardness and elastic limit, considerable fatigue strength and exceptional resistance to wear and deformation, so it is specified by precision bearing producers where spherical and tolerance accuracy is essential. In the as-cast state, its microstructure is lamellar pearlitic. After austenitizing and rapid quenching, it exhibits a martensitic structure; considerable contents of retained austenite can remain besides the martensitic microstructure in the final material. The volume content and the stability of this retained austenite influence the fatigue limit of the considered material [18]. Slow cooling from the freezing range reduces the amount of this retained austenite, recovering toughness properties [20]. Another important characteristic of the considered material is its good hardenability: hardening should allow oil quenching to minimize the risk of hardening cracks or distortions and to reduce to the minimum the successive grinding procedures.

The stability of the austenite in the context of martensitic transformation at lower temperatures for this material depends mostly on C and Cr contents [20]. Other properties of this material can be found, e.g., in [21]. Micrographs of this steel as hardened and tempered, exhibit the martensitic matrix with high content of C and carbides diffused in the mass.

The heat treatment procedure for the considered ring is carried out through the following consecutive steps: austenitizing reheating at 850–860 °C; oil quenching at ∼ 90 °C, in order to create martensite; tempering by reheating in air furnace at ∼ 200 °C to decrease hardness and stabilize the part. The main aims of the adopted heat treatment are: to create adequate strength gradients to withstand the stress gradients and supply a satisfactory safety level; to produce a fine martensitic microstructure; to increase hardness according to the penetration of the martensitic transformation in the part section; to eliminate surface wear as much as possible.

2.2. Neutron diffraction for residual stress measurements

Neutrons, in the case of ND measurements on polycrystalline samples, are sensitive to the crystalline structure and its changes. RS are not measured directly but they are calculated from measurement of residual strains, which are then converted to stresses using appropriate moduli. The neutrons from the sample gauge volume are diffracted by a family of lattice planes (hkl) under the $2\theta_{hkl}$ scattering angle, according the Bragg's law:

$$2d_{hkl}\sin\theta_{hkl} = \lambda, \tag{1}$$

where d_{hkl} is the measured interplanar spacing, θ_{hkl} is the Bragg's angle – i.e., one-half the scattering angle for a diffraction peak corresponding to the crystallographic Miller indices (h, k, l) – and λ is the neutron wavelength.

The differentiated Bragg's equation gives a relative lattice strain ε_{hkl} in the form:

$$\varepsilon_{hkl} = \frac{d_{hkl} - d_{0,hkl}}{d_{0,hkl}} = \frac{\Delta d_{hkl}}{d_{0,hkl}} = -\cot\theta_{hkl}\Delta\theta_{hkl}, \tag{2}$$

where $d_{0,hkl}$ is the stress-free interplanar spacing.

The strain determination is based on measurements of angular deviation $\Delta\theta_{hkl}$ of the diffraction profile position from the value related to the stress-free state. The analysis of tri-axial stress states, in general, requires accurate values of the unstressed interplanar spacing. A strain free sample of the material avoids systematic errors in the $d_{0,hkl}$ – and hence in the strain value – and various experimental and analytical methods exist for the determination of $d_{0,hkl}$, which are discussed in [22]. In fact, one neutron diffraction measurement provides a value of the strain component $\varepsilon^{hkl}_{x,y,z}$ parallel to the scattering vector $\boldsymbol{Q}$ (Fig. 2), which is perpendicular to the set of diffracting planes (hkl).

The stress component σ_x can be obtained, consequently, by knowing the diffraction elastic Young's modulus E_{hkl} and the diffraction Poisson's ratio ν_{hkl} of the considered material, and using the Hooke's law in the form:

$$\sigma_x = \frac{E_{hkl}}{(1-2\nu_{hkl})(1+\nu_{hkl})} \cdot \cdot [(1-\nu_{hkl})\varepsilon^{hkl}_x + \nu_{hkl}(\varepsilon^{hkl}_y + \varepsilon^{hkl}_z)], \tag{3}$$

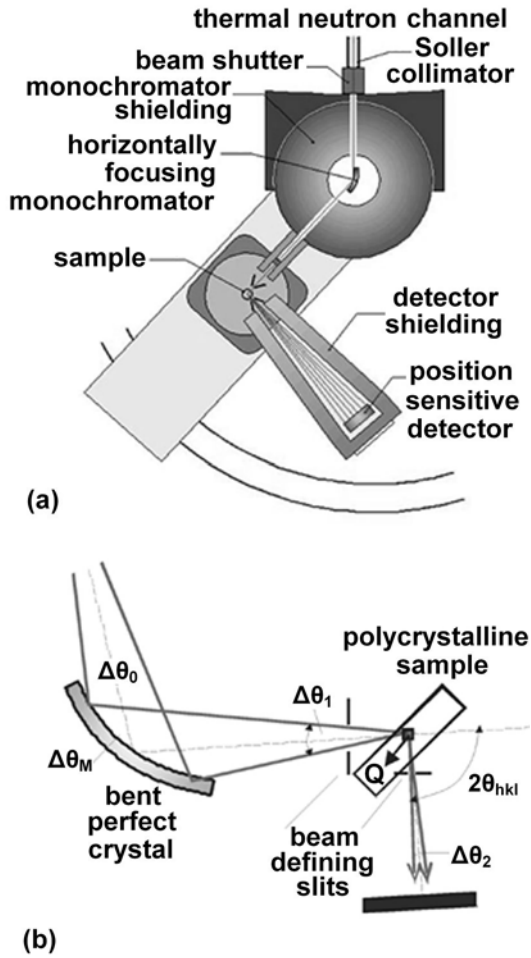

Fig. 2. Schematic layout of the double axis diffractometer adopted for the stress investigation (a) and detailed geometry of the diffractometer focusing performance (b). $\boldsymbol{Q}$ is the scattering vector perpendicular to the diffraction lattice planes.

where $\varepsilon^{hkl}_{x,y,z}$ is the x-, y-, z-component of the lattice strain measured on the crystal lattice planes (hkl). Corresponding relations for other y and z stress components are obtained by simple permutations of x, y and z indices. The mapping of residual strains can be carried out with reference to the radial, hoop and axial stress directions shown in Fig. 1c, which for application of the formula (3) corresponded to x, y and z directions, respectively.

The sample gauge volume is defined by using two fixed slits in the incident and diffracted beam, respectively. The specimen is moved step by step in the z direction and the corresponding diffraction spectra are collected in each position. The corresponding component of the strain tensor is adjusted by a proper rotation of the specimen with respect to the scattering vector $\boldsymbol{Q}$.

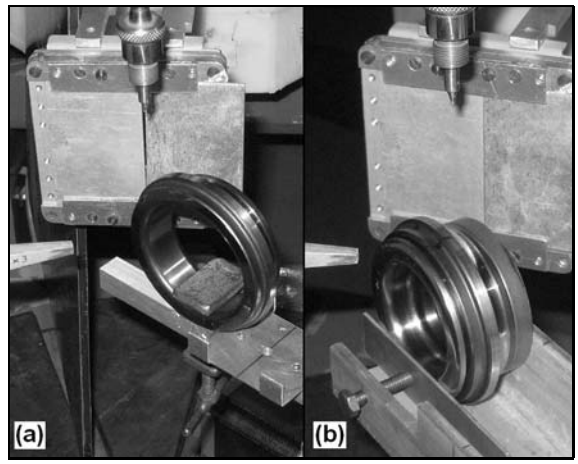

Fig. 3. The free ring (a) and the same ring with the hub introduced (b), during the ND measurements.

3. Experimental procedures and results

The measurements were carried out by using the strain scanning neutron diffractometer of the medium power reactor LVR-15 in Řež (see the scheme in Fig. 2).

This diffractometer, particularly suitable for macro/micro strain scanning of polycrystalline materials, exploits advantages coming from focusing both in real and momentum space and yields good resolution and luminosity, especially for samples of small dimensions [23–25]. In the strain scanning by this diffractometer, the gauge volume is determined by two fixed Cd slits – (2–5) × (3–30) mm^2 – in the incident and diffracted beams, and the measurements are usually performed in the vicinity of the scattering angle $2\theta_{hkl} = 90°$. For these values of $2\theta_{hkl}$, the typical uncertainty in determining the strain is slightly better than 10^{-4}.

In our case, the neutron wavelength of $\lambda = 2.35$ Å was used, which for Fe(110) reflection determines the scattering angle $2\theta_{110} = 70°$. The following elastic and Poisson's constants were employed: $E = 225.5$ GPa; $\nu = 0.28$. These constants correspond to those calculated using the Kröner's model, taking into account the anisotropy function of the considered material. By using a gauge volume of $1 \times 1 \times 1.5$ mm^3, different sample spatial positions were investigated along the line A-B as indicated in Fig. 1. Figure 3 shows the photos of the free ring (a) and the ring completed with the hub (b) during the measurements.

Figures 4 and 5 show respectively the obtained residual strain and stress components with reference to the free ring (a), the same ring completed with the hub (b), and the second ring completed earlier (c). The scanning carried out in the free ring has provided first result indicating that the interplanar distance d

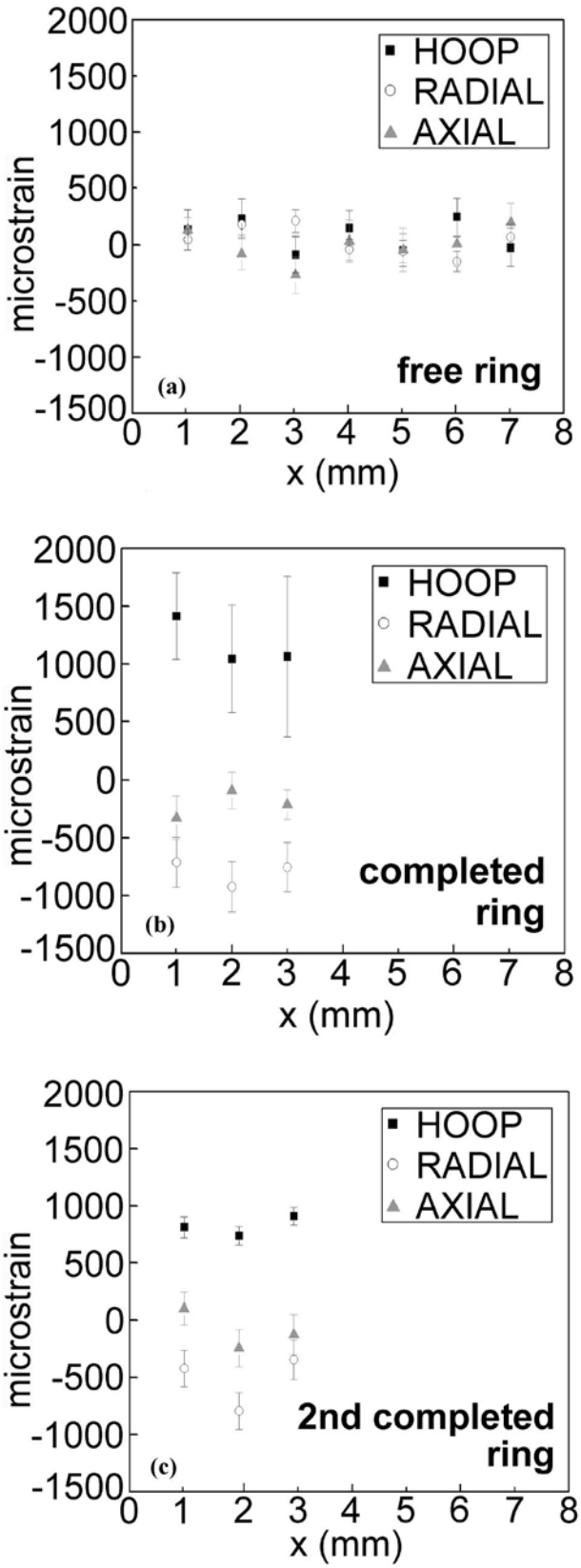

Fig. 4. The measured strains, with reference to the free ring (a), the same ring with the hub introduced (b), and the second ring with the hub introduced (c).

(value averaged within the gauge volume) remains in the measurement points nearly unchanged. d_0 value was taken from the measurement on the free ring in the place deep (far from the surface) in the material, where the values of $\Delta\theta$ for all three components did not change. Some modest variations of d in the measurement points on the line A-B and, consequently, the low values of the obtained strain values for the free ring, can be attributed predominantly to the geometrical features of the specimen. It results in low level stresses shown for the free ring in Fig. 5a (in the range from $\sim$ –65 MPa to $\sim$ 75 MPa) and the sample can be considered as a relaxed sample and nearly homogeneous for all the three measurement directions (hoop, radial and axial). It should be pointed out that in the case of the free ring the measurement could be carried out up to the depth of 7 mm, while in the case of completed rings it could be only to the depth of 3 mm.

4. Discussion

First of all it should be pointed out that all components of the residual strain/stresses were measured in the free ring and no RS level was observed within the experimental errors (Figs. 4a and 5a). Therefore, in order to emphasize the residual strain/stress effects due to the introduction of the hub and the successive rolling operation, the strain/stress state before these operations (i.e., related to the free ring, as shown in Fig. 4a) was taken as a reference for the determination of the RS in both the completed rings (Figs. 4b,c and 5b,c). These RS were calculated (see Eq. (3)), thus, employing the difference between the strain states preceding and successive of joining and rolling; they represent their real values due to the effects of these operations. Strain and residual stress trends are similar for both the completed rings. Naturally, higher residual strains and stresses are tensile components along the hoop direction and their status is practically due to the introduction of the hub, which creates a load in the ring material.

In particular, for the first completed ring (Fig. 5b): the hoop RS component, from a tensile value of $\sim$ 300 MPa in correspondence with the first sub-surface gauge volume (corresponding to the point A of Fig. 1c), decreases to $\sim$ 200 MPa in both adjacent gauge volumes (direction AB in Fig. 1c); as can be expected, the values of axial RS components are roughly zero within the experimental errors for all three investigated gauge volumes; the radial RS component begins from a compressive value of $\sim$ –75 MPa in correspondence with the first sub-surface gauge volume, then decreases to $\sim$ –150 MPa in correspondence with the adjacent gauge volume, and goes back to $\sim$ –100 MPa for the last gauge volume investigated. Before doing some specific conclusions, however, rather large exper-

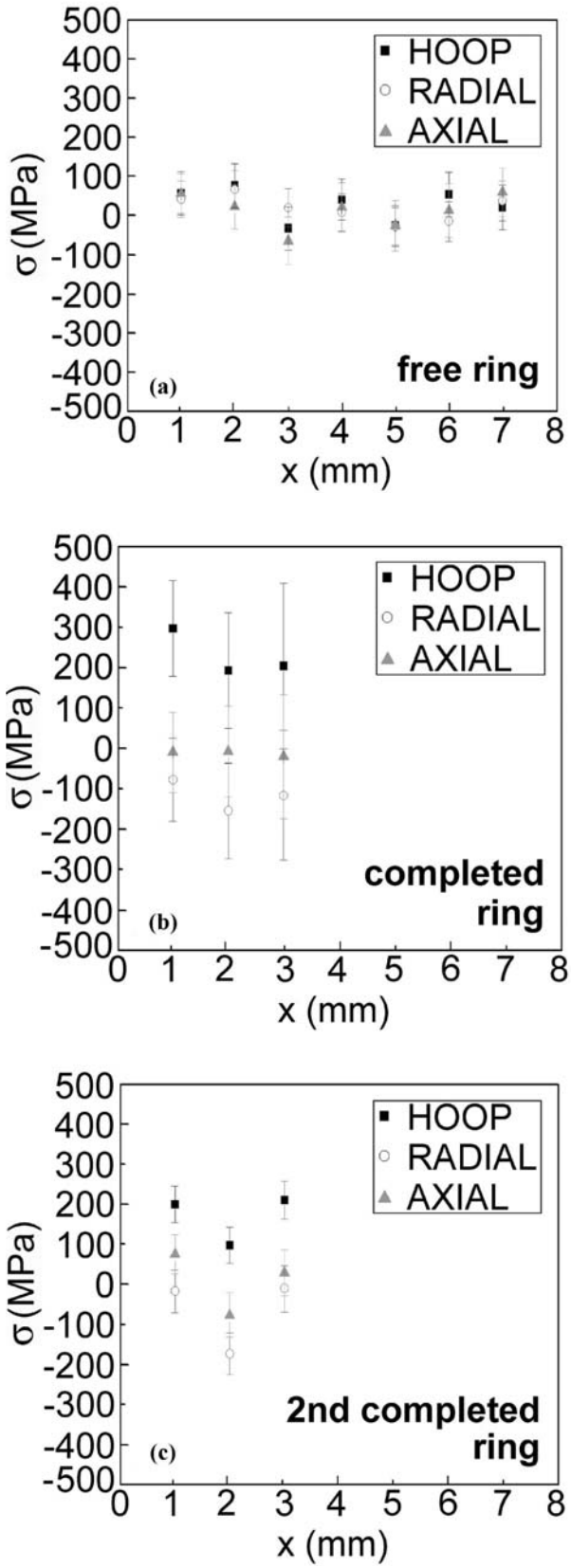

Fig. 5. The determined residual stresses with reference to the free ring (a), the same ring with the hub introduced (b), and the second ring with the hub introduced (c).

imental errors brought about by much worse statistics with respect to the second completed ring, should be considered. Therefore, some small stress component alterations between the individual measurement points have no special meaning. Namely, large experimental errors of the hoop strain components (Fig. 5b) of the first completed ring resulted after calculation also in rather large errors of all stress components.

For the second completed ring (Fig. 5c): the hoop RS component, from a tensile value of $\sim$ 200 MPa in correspondence with the first sub-surface gauge volume, decreases to $\sim$ 100 MPa for the adjacent volume and goes back up to little more than 200 MPa for the last gauge volume investigated; the axial RS component, from a tensile value of $\sim$ 75 MPa in correspondence with the first sub-surface gauge volume, decreases to $\sim$ –75 MPa for the adjacent volume and goes back roughly to zero for the last gauge volume investigated; the radial RS component, from a value being close to zero in correspondence of the first sub-surface gauge volume, decreases to $\sim$ –170 MPa for the adjacent volume and returns to almost zero for the last investigated gauge volume. The mentioned values are averaged within the respective gauge volume investigated. Also in this case some alterations in the values of individual components for three investigated measurement points have no special meaning.

The lower detector signal resulted in worse statistics in the case of the first completed ring with respect to the second one can be explained by a slightly different microstructure brought about by a slightly different material processing (it can produce, e.g., the presence of higher amount of martensite phase, a difference in plasticity status, etc.). Nevertheless, the RS level in both samples is comparable (Fig. 5b,c).

5. Conclusions

Neutron diffraction has proved to be a very efficient tool for monitoring residual stresses. In many cases it also appears very suitable for verifying predictions of FEM simulations. The presented results demonstrate measurement feasibility and the industrial applicability of the neutron diffraction technique in the bearings sector. The obtained data are easy to interpret: they supply indications that can be taken into account as possible reference in determining strains and residual stresses in bearing rings made of the required or similar materials. The measurement can be carried out starting from the surface and the sub-surface to several millimetres in depth. The achieved results could be useful for: obtaining an information how to enhance the knowledge of the involved material; an evaluation of its characteristics and behaviour; an indication on the effects of heat treatment and monitoring its features; a support in the life assessment of

the component; a contribution to the enhancement of FEM calculations. Therefore, they can be exploited to optimize the operative conditions and/or modify the heat treatment parameters, with the purpose of achieving the most appropriate residual stress gradients and, thus, in the perspective to help in developing advanced ring production technologies. Of course, a complementary micro- and nano-structural characterization by small-angle neutron scattering, which allows monitoring key parameters as, e.g., size and concentration of inhomogeneities (micro- and nano--defects such as precipitates-carbides and voids), their volume fraction and interface area would be desirable. The mentioned parameters can superimpose with the residual stress status and they can make worse the risk of cracks during the straightening of the ring. All this can help the manufacturer to enhance the quality of the heat treatment and other necessary procedures, and thus, to support the life assessment of the component. Finally, it can be stated that the applicability of neutron diffraction technique in engineering offers significant information usually not available by any other method.

Acknowledgements

The research has been conducted at the CANAM (Center of Accelerators and Nuclear Analytical Methods LM2011019) infrastructure with a funding from the Ministry of Education, Youth and Sports of the Czech Republic.

References

[1] Ebert, F. J.: Chinese Journal of Aeronautics, *23*, 2010, p. 123. doi:10.1016/S1000-9361(09)60196-5
[2] Lacarac, V., Chang, C. C., Bramley, A. N., Tierney, M. J., McMahon, C. A., Smith, D. J.: Proceedings Inst. Mech. Eng., Part B: J. Eng. Manuf., *219*, 2008, p. 301.
[3] Ericsson, T.: In: Handbook of Residual Stress and Deformation of Steel. Eds.: Totten, G., Howes, M., Inoue, T. Materials Park, ASM International 2002, p. 151.
[4] Surm, H., Kessler, O., Hoffmann, F., Mayr, P.: Int. J. Mater. Prod. Technol., *24*, 2005, p. 270. doi:10.1504/IJMPT.2005.007954
[5] Robelet, M., Rassili, A., Fischer, D.: J. Solid State Phenom., *116/117*, 2006, p. 712. doi:10.4028/www.scientific.net/SSP.116-117.712
[6] Ryttberg, K., Knutson Wedel, M., Recina, V., Dahlman, P., Nyborg, L.: Mater. Sci. Eng., A, *527*, 2010, p. 2431. doi:10.1016/j.msea.2009.12.016
[7] Epp, J., Surm, H., Kessler, O., Hirsch, T.: Acta Mater., *55*, 2007, p. 5959. doi:10.1016/j.actamat.2007.07.022
[8] Rogante, M.: In: Proceedings 1st Italian Workshop for Industry Applicazioni Industriali delle Tecniche Neutroniche®. Ed.: Rogante, M. Civitanova Marche, Italy, Rogante Engineering 2008, p. 40.
[9] Rogante, M., Rosta, L.: In: Proceedings of SPIE 5824, Opto-Ireland 2005: Nanotechnology and Nanophotonics. Eds.: Blau, W. J., Kennedy, D., Colreavy, J. Bellingham, WA, SPIE 2005, p. 294.
[10] Rogante, M.: Oil Gas J., *103*, 2005, p. 59.
[11] Rogante, M.: In: Proceedings MATRIB '03. Ed.: Grilec, K. Zagreb, Croatian Society for Materials and Tribology 2003, p. 235.
[12] Rogante, M., Mikula, P., Vrána, M.: Key Eng. Mat., *465*, 2011, p. 259. doi:10.4028/www.scientific.net/KEM.465.259
[13] Epp, J., Surm, H., Hirsch, T., Hoffmann, F.: J. Mater. Process. Techn., *211*, 2011, p. 637. doi:10.1016/j.jmatprotec.2010.11.022
[14] Amey, C. M., Huang, H., Rivera-Díaz-Del-Castillo, P. E. J.: Mater. Design, *35*, 2012, p. 66. doi:10.1016/j.matdes.2011.10.008
[15] Nallathambi, A. K., Kaymak, Y., Specht, E., Bertram, A.: J. Mater. Process. Techn., *210*, 2010, p. 204. doi:10.1016/j.jmatprotec.2009.09.001
[16] Perez, M., Sidoroff, C., Vincent, A., Esnouf, C.: Acta Mater., *57*, 2009, p. 3170. doi:10.1016/j.actamat.2009.03.024
[17] Kerscher, E., Lang, K. H.: J. Phys.: Conference Series, *240*, 2010, p. 012059. doi:10.1088/1742-6596/240/1/012059
[18] Desvaux, S., Duquennoy, M., Gualandri, J., Ourak, M.: NDT & E Int., *37*, 2004, p. 9. doi:10.1016/S0963-8695(03)00046-X
[19] Bhadeshia, H. K. D. H.: Progress in Mater. Sci., *57*, 2012, p. 268. doi:10.1016/j.pmatsci.2011.06.002
[20] Püttgen, W., Hallstedt, B., Bleck, W., Löffler, J. F., Uggowitzer, P. J.: Acta Mater., *55*, 2007, p. 6553. doi:10.1016/j.actamat.2007.08.010
[21] MatWeb Materials Property Database, http://www.matweb.com
[22] Rogante, M.: Phys. B, *276–278*, 2000, p. 202. doi:10.1016/S0921-4526(99)01281-8
[23] Mikula, P., Vrána, M., Lukáš, P., Šaroun, J., Wagner, V.: Mater. Sci. Forum, *228/231*, 1996, p. 269. doi:10.4028/www.scientific.net/MSF.228-231.269
[24] Mikula, P., Wagner, V.: Mater. Sci. Forum, *347/349*, 2000, p. 113. doi:10.4028/www.scientific.net/MSF.347-349.113
[25] Vrána, M., Mikula, P.: Mater. Sci. Forum, *490/491*, 2005, p. 234. doi:10.4028/www.scientific.net/MSF.490-491.234